

Multifractal structure and intermittence in the AE index time series (*)

G. CONSOLINI and M. F. MARCUCCI

*Istituto di Fisica dello Spazio Interplanetario, CNR
Via Fosso del Cavaliere, 00133 Roma, Italy*

(ricevuto il 4 Aprile 1996; approvato il 24 Maggio 1996)

Summary. — The conventional approach to magnetospheric dynamics has not provided until now a satisfactory description of the singular behaviour of magnetospheric substorms. In this paper we present a multifractal analysis of AE time series, based on *singularity analysis*, a new tool to investigate signal dynamics features. The existence of a multifractal structure of the AE index with respect to *time dilation* has been investigated. The resulting multifractal behaviour of the signal can be interpreted as the signature of an underlying *intermittence phenomenon*. The derived *singularity spectrum* is well in agreement with the one of a two-scale Cantor model (*P-model*), a pure multiplicative model. The presence of intermittence in AE might indicate the occurrence of *turbulence* in magnetospheric dissipation processes.

PACS 94.20 – Physics of the ionosphere.

PACS 94.30.Lr – Magnetic storms, substorms.

PACS 01.30.Cc - Conference proceedings.

1. – Introduction

A fully comprehensive model of magnetospheric dynamics has not been developed yet. The conventional approach, based on the solution of the magnetohydrodynamic equations with *ad hoc* boundary conditions, does not provide a satisfactory description of the irregular behaviour of the magnetospheric substorms. Furthermore, the solar wind, which surely drives magnetospheric processes, is a highly turbulent plasma flow, and displays a multifractal structure when large-scale fluctuations of the interplanetary magnetic field, IMF, are considered [1]. The main manifestations of the interaction between the solar wind and the magnetosphere are the magnetospheric substorms, which represent a global response of the magnetosphere to changes of the

(*) Paper presented at the VII Cosmic Physics National Conference, Rimini, October 26-28, 1994.

solar wind conditions. The evolution of these substorms is very irregular, and this irregularity may be related to low-dimensional chaos [2-11].

The magnetospheric response to the solar wind can be described by several geomagnetic indices. Among these the Auroral Electroject Index (AE), a measure of the horizontal current strength flowing in the lower ionosphere, is an indicator of the energy dissipation processes due to solar wind-magnetosphere interaction [12].

Recently, the possibility that the irregular magnetospheric behaviour may be due to chaotic dynamics has been investigated taking into account the progress in the characterisation of dissipative non-linear dynamical systems that display chaotic dynamics. The majority of these studies concerns the time behaviour of the AE index and the occurrence of chaos in it [7, 10, 11].

Here we present a new study of the AE time series properties, based on the multifractal approach and on the analysis of the probability distribution function of the signal gradients (PDF).

We propose a *P-model* (*two-scale Cantor set*) in order to explain the *singularity spectrum* and the hierarchy of the *generalised dimensions*.

The existence of a multifractal nature with respect to *time dilation* must be regarded as a characterisation of the underlying *intermittence phenomenon*.

2. – Data sets and analysis

2.1. Data description. – In the present paper we focus our attention on the Auroral Electroject activity index (AE). It was introduced by Sugiura and Davis [12] as a measure of the total maximum amplitude of the electroject currents.

As shown by Akasofu [13], a relationship exists between the energy consumption rate of the magnetosphere and the AE index. Furthermore, there is a good correlation between the input energy flux responsible for the magnetospheric substorms and storms, and AE. So we can conclude that the AE index is a significant descriptor of the magnetospheric response to solar wind changes. Moreover, AE time series are characterised by a high temporal resolution and by measurement continuity.

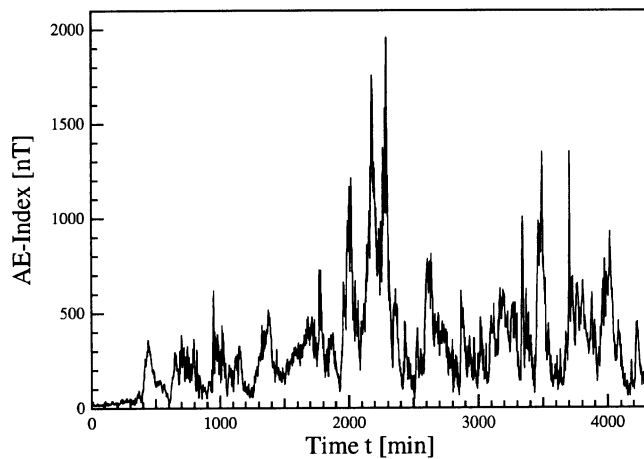


Fig. 1. – Sample of the original time series, covering a period of 3 days.

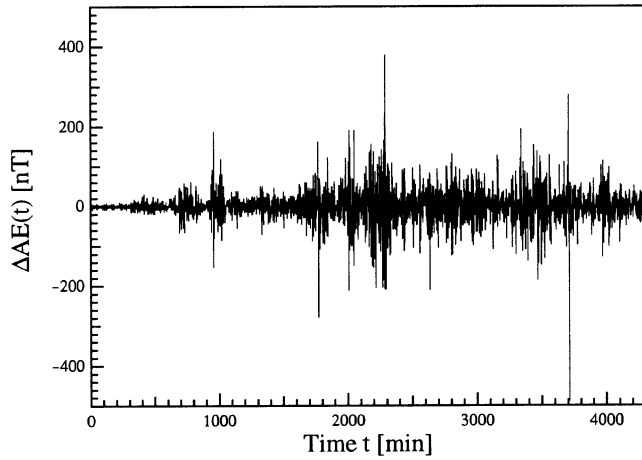


Fig. 2. – Time series of AE data increments for the same period as in fig. 1.

In our analysis, without any preliminary assumption, we have considered a time series of 2^{16} points, covering the period from 01/01/1975 to 19/02/1975, with 1-minute time resolution for the *multifractal approach* and a time series covering the whole year 1975 for the evaluation of the *probability distribution function* (PDF) of the signal gradients. Data, available on CD-ROM [NGDG-05/1], come from the National Geophysical Data Centre, Boulder, Colorado, USA.

In fig. 1, a segment of 3 days (4320 points) of the original time series is shown. In this figure it is evident that large and sharp bursts occur in the temporal evolution of the AE signal. This *spotty* behaviour, which is more evident in the small-scale increments of the data (see fig. 2), may suggest the occurrence of intermittence, and consequently of turbulence.

2.2. Spectral analysis. – The study of the AE signal has been started with the analysis of its spectral features. In fig. 3, we report the power spectral density (PSD) $S(f)$ of the total time series, computed using Welch's modified periodogram method. In order to reduce the aliasing problem, we have used a windowing procedure; the used window was a BlackmanHarris3 - 3 term (67 dB).

The main feature of the PSD is its broad-band nature; in fact there are no spikes at any characteristic frequency, apart from the outstanding one at $f \approx 1.2 \cdot 10^{-5}$ Hz (≈ 24 h), which was already observed by Tsurutani *et al.* [14]. Furthermore, it is possible to identify two spectral breaks, one at $f_1 = 7.34 \cdot 10^{-5}$ Hz, already observed in several works [14], and another at $f_2 = 2.47 \cdot 10^{-3}$ Hz. Consequently, the PSD can be separated into three regions, each of which can be described by a power law

$$(1) \quad S(f) = Af^{-\alpha},$$

with a different α .

The analysis of the spectral exponent suggests that the AE signal is nearly stationary ($\alpha \approx 1$) at low frequency (long time scales), and non-stationary with stationary increments ($1 < \alpha < 3$) at intermediate and high-frequency (intermediate

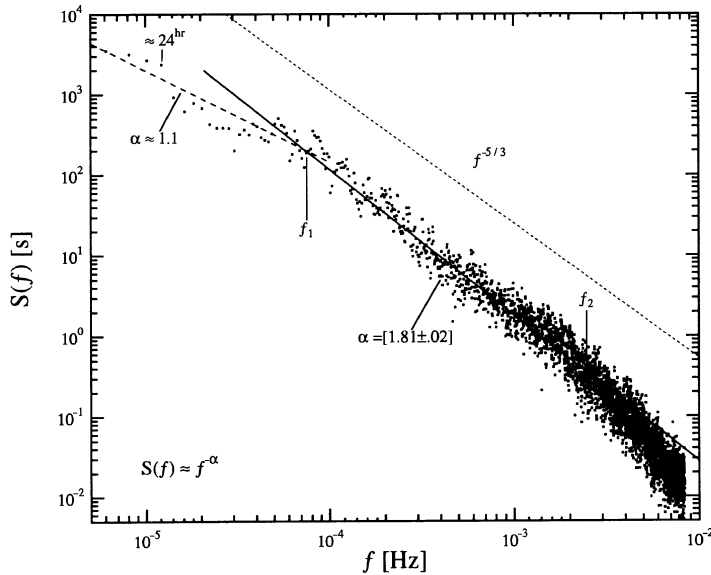


Fig. 3. – Power spectral density (PSD) relative to the period under analysis. The solid line and the long-dashed line are power law best fits. The short-dashed line is relative to the $-5/3$ power law predicted by Kolmogorov's theory. f_1 and f_2 are the two spectral breaks that identify the so-called *pseudo-inertial range*.

and short time scales) [15]. With the word *stationarity* we mean the statistical invariance of the signal by a translation in time (*ergodicity*).

The nearly stationary region may be the consequence of a limitation of large-scale fluctuations, required to maintain the signal within a physically accessible range. On the other hand, the steeper non-stationary region at higher frequency has to be correlated with the smooth behaviour at smaller time scales.

So we can conclude that the spectral features of the AE index signal are those of a non-stationary signal with stationary increments over a range of scales, bounded below and above. This range may be evaluated from the two spectral breaks as the associated half-period

$$(2) \quad 3' \leq t \leq 120'.$$

Using Taylor's hypothesis

$$(3) \quad l = \tau V_f,$$

where V_f is the velocity of the flow, so that

$$(4) \quad k \Rightarrow f;$$

we have shown the typical $-5/3$ Kolmogorov's power spectrum in fig. 3.

If we assume that our signal is due to a turbulent flow, the above-identified range seems to be comparable with the usual inertial range in turbulence; we will call it *pseudo-inertial range*. Furthermore the small discrepancy between the $-5/3$ power spectrum and the observed one may be a consequence of *intermittence*.

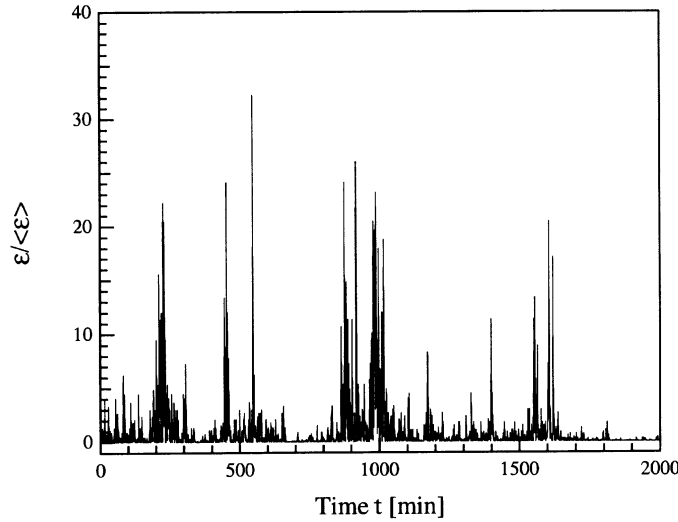


Fig. 4. – Example of the new-scalar field $\varepsilon(t)$ defined on the original AE data set.

2.3. Multifractal analysis. – The purpose of multifractal analysis is to quantify the various scaling indices, which are the natural consequence of the different local scaling properties of the data. In order to do this, the first step is the definition of a positive stationary singular measure on the data-set [15, 16].

Since the AE signal is not stationary, we first derive a stationary non-negative field from it defining a new scalar field $\varepsilon(t)$, as the squared absolute value of the small-scale differences ($\Delta t = 1$ min), according to Meneveau and Sreenivasan [17]:

$$(5) \quad \varepsilon(t) = [\varphi_{AE}(t_i + \Delta t) - \varphi_{AE}(t_i)]^2,$$

where $\varphi_{AE}(t)$ represents the original AE signal.

Figure 4 shows an example of the behaviour of $\varepsilon(t)/\langle\varepsilon(t)\rangle$ covering a period of 2000 minutes.

We have defined a measure $d\mu$ on this new field

$$(6) \quad d\mu(t) = \frac{\varepsilon(t)}{\langle\varepsilon\rangle T} dt,$$

where T is the total time length, which is consequently a positive stationary measure.

A multifractal measure is characterised by the scaling of the corresponding coarse-grained weight

$$(7) \quad p_i(\tau) = \int_{\Lambda_i} d\mu(t) \approx \sum_{t'=t_i}^{t_i+\tau-1} \Delta\mu(t'),$$

where the set supporting the measure has been partitioned in segments Λ_i , of size τ . The signature of multifractality is in the anomalous power law of the *partition function*

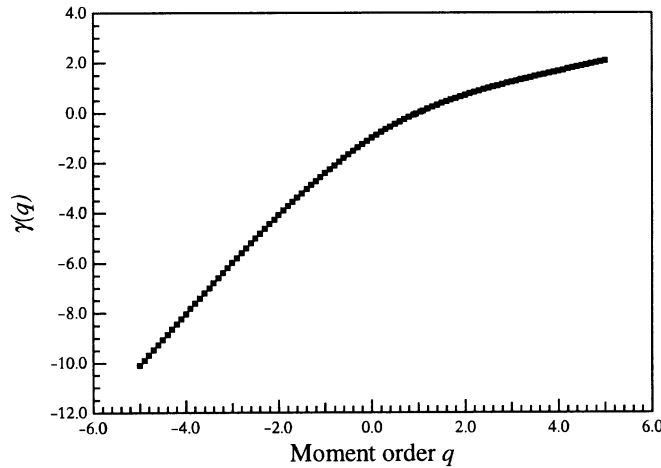


Fig. 5. – Scaling exponent $\gamma(q)$ of the *partition function* $\Gamma(q, \tau)$ as a function of the moment order q .

$\Gamma(q, \tau)$ for small τ :

$$(8) \quad \Gamma(q, \tau) = \sum_{\Lambda_i} p_i(\tau)^q \approx \tau^{\gamma(q)},$$

where $\gamma(q) = (q - 1) D_q$, with a non-constant function D_q .

The exponents D_q are called *generalised dimensions* and according to Hentschel and Procaccia [18] D_0 is the fractal dimension of the support of the measure, D_1 the information dimension and D_2 the so-called correlation dimension.

Now, if the fractal is homogeneous, the D_q dimensions are all equal to the fractal dimension D_0 and therefore $\gamma(q)$ has a linear dependence on q .

In order to evaluate the $\gamma(q)$ exponents, for each q in the range $[-5, 7]$ we set τ as

$$(9) \quad \tau = 2^n \Rightarrow n \in N, \quad 4 \leq n \leq 8$$

in the last expression of $\Gamma(q, \tau)$.

The resulting $\Gamma(q, \tau)$ vs. τ has been fitted with a power law using the Levenberg-Marquardt non-linear regression algorithm. The use of a non-linear regression method is a very crucial point in this type of analysis; in fact the use of linear methods, as log-log best fit, introduces some spurious results.

Figures 5 and 6, respectively, show the resulting values for $\gamma(q)$ and D_q as a function of q .

It is evident in fig. 5 that the dependence of $\gamma(q)$ on q is not linear, and this is due to the underlying multifractal structure of the AE signal. Furthermore, the observed dependence of D_q on q is the signature of the existence of a hierarchy of dimensions, and this is typical for a multifractal measure. In order to investigate the nature of the temporal dishomogeneity of the signal, we have compared the D_q curve with that of a typical multiplicative process, the “*P-model*”, introduced by Meneveau and Sreenivasan [17] to explain the intermittent character in turbulent fluid flows.

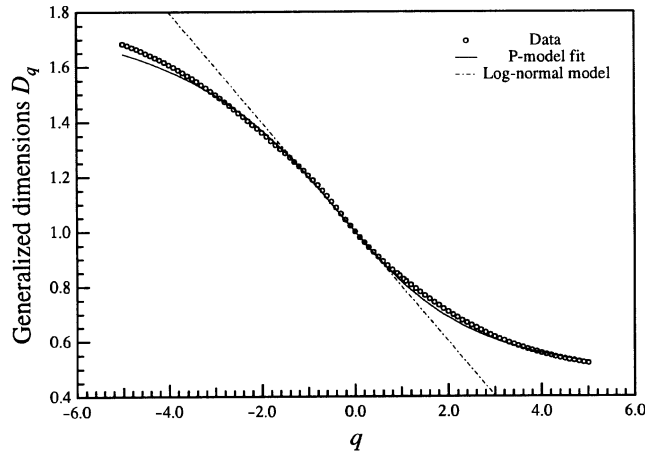


Fig. 6. – Plot of the *generalised dimension* D_q . The solid line is the non-linear best fit of the data by the *P-model* (see text at expression (10)). The dot-dashed line represents the behaviour of D_q in the case of the *log-normal model*.

The solid line in fig. 6 represents the non-linear best fit of the D_q data using the *P-model*:

$$(10) \quad D_q = \log_2 [p^q + (1 - p)^q]^{1/(1-q)},$$

where

$$(11) \quad p = [0.746 \pm 0.002].$$

The agreement is excellent, and the resulting parameter p can be used to compute the *intermittence exponent*

$$(12) \quad \mu = -2 \left. \frac{dD_q}{dq} \right|_{q=0} = \log_2 [4p(1-p)]^{-1},$$

$$(13) \quad \mu = [0.400 \pm 0.002].$$

From the knowledge of the intermittence exponent μ it is possible to evaluate the correction to the PSD in the inertial range. In fact

$$(14) \quad f^{-\beta} \xrightarrow{\text{intermittence correction}} f^{-\beta - \mu/3} = f^{-\alpha},$$

so that, if $\beta = 5/3$ we obtain

$$(15) \quad \alpha = [1.800 \pm 0.001],$$

which is well in agreement with the experimental result on PSD in the so-defined *pseudo-inertial range*.

Another way to characterise the multifractality is given by the so-called *multifractal* or *singularity spectrum* $f(\alpha)$. This description is equivalent but allows to emphasise certain physical aspects. In particular, this formalism leads to the

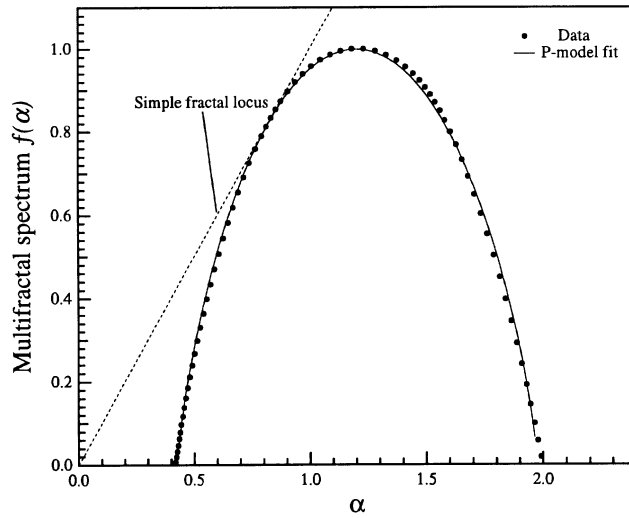


Fig. 7. – *Multifractal spectrum or singularity spectrum* $f(\alpha)$. The solid line is the non-linear best fit of the data by the expression (17) relative to a *two-scale Cantor set (P-model)*.

description of a multifractal measure in terms of interwoven sets of Hausdorff dimension $f(\alpha)$ with singularity strength α .

Now it is possible to evaluate the $f(\alpha)$ directly from the $\gamma(q)$ curve by a Legendre transformation

$$(16) \quad \alpha = \frac{d\gamma(q)}{dq}, \quad f(\alpha) = q\alpha - \gamma(q).$$

In the limit of a homogeneous support for the measure the singularity spectrum is defined only for $\alpha = D_0$ implying $f(D_0) = D_0$, while in the case of a multifractal support the result is generally a convex curve.

In fig. 7 we report our result for the *singularity spectrum* $f(\alpha)$. The straight line is the diagonal $f = \alpha$ that corresponds to the special case of a simple fractal.

In agreement with the previous result we found that the *singularity spectrum* is well fitted by the resulting multifractal spectrum for a general *two-scale Cantor set*, obtained by Halsey *et al.* [19]:

$$(17) \quad \begin{cases} \alpha = - \frac{\log_2 p_1 + (n/m - 1) \log_2 p_2}{n/m}, \\ f(\alpha) = - \frac{(n/m - 1) \log_2(n/m - 1) - (n/m) \log_2(n/m)}{n/m}, \end{cases}$$

from which it is possible to obtain a direct expression for $f(\alpha)$.

This expression has been written for a *two-scale Cantor set* with equal scales but unequal weights, which is equivalent to the *P-model*.

Once again a good agreement is found with the experimental data.

2.4. *Probability distribution function (PDF) of the signal gradient.* – The presence of intermittence can be directly checked through the study of the probability distribution function (PDF) of the signal gradient. In fact, the non-Gaussian shape of the PDF at small scales corresponds to the presence of strong intermittence in the signal.

In panel a) of fig. 8 we have reported the PDF for two different time scales

$$(18) \quad \tau = 1 \text{ min} , \quad \tau = 8 \text{ h} ,$$

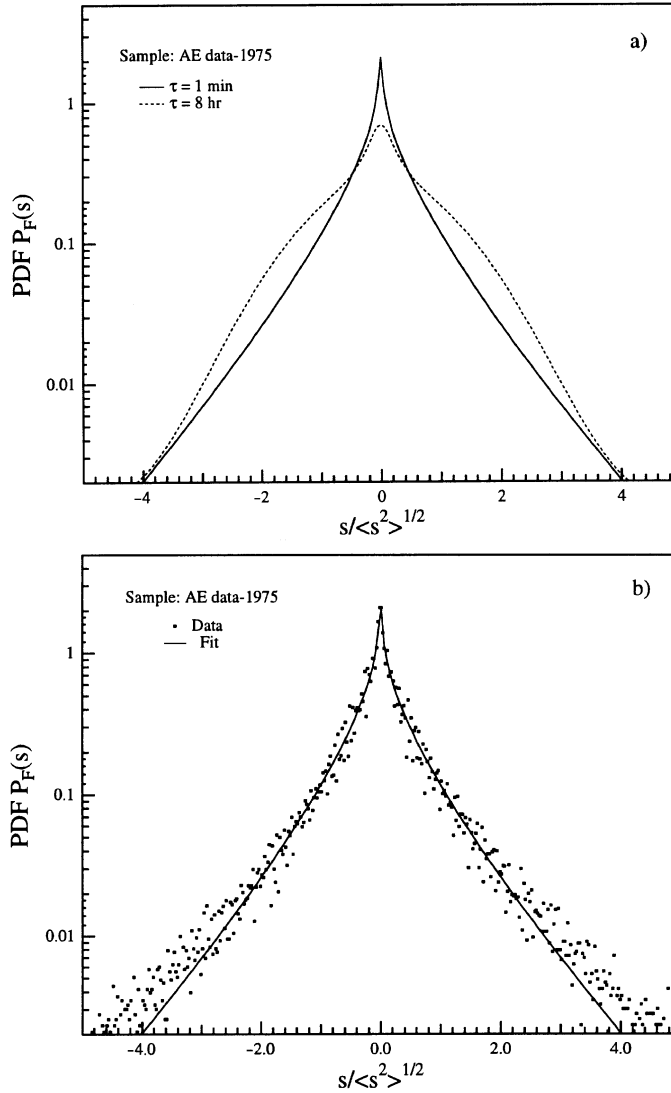


Fig. 8. – Probability distribution function (PDF) of the signal gradient. Panel a) shows the PDF for two different time scales. Panel b) shows the comparison between PDF at shortest scale and Kraichnan's approximation (see text at expression (19)). Kraichnan's approximation (solid line) is a non-linear best fit of the PDF data.

where, in order to compute the PDF at larger scale we have extended the statistics to the whole year 1975.

The shape at smaller scale is clearly non-Gaussian, since it becomes more peaked around zero with relatively high tails, corresponding to the presence of strong *intermittence* in the signal gradient and hence in the scalar field $\varepsilon(t)$.

In panel b) of the same figure we compare the resulting non-Gaussian shape of the PDF at the smallest scale with the approximation used from several authors [20-22]:

$$(19) \quad P(\xi) \approx \xi^\gamma e^{-\beta|\xi|^\alpha},$$

where

$$(20) \quad \xi = \frac{s}{\langle s^2 \rangle^{1/2}} \Rightarrow s = \Delta\varphi_{\text{AE}}(\tau),$$

with $\Delta\varphi_{\text{AE}}(\tau)$ the differenced time series on scale τ . The agreement with theory is very good.

3. – Concluding remarks

The study of the spectral and scaling features of the AE index has evidenced the existence of a multifractal structure of the signal. The multifractality with regard to the time dilation is the signature of the presence of a temporal dishomogeneity. Furthermore, dishomogeneity in the sense of singular measures is the currently accepted way of making the concept of *intermittence* precise, so it is possible to conclude that the AE signal is characterised by an *intermittence phenomenon*.

Moreover, the existence of a multifractal measure indicates an underlying multiplicative process leading to it; such multiplicative process is well confirmed by the good agreement between our data and the *P-model*.

Furthermore, the presence of *intermittence* is also confirmed by the analysis of the PDF of the signal gradient.

From a physical point of view, the occurrence of *intermittence* in the AE signal may be an indication of the presence of *turbulence*. On the other hand, the characteristic range of scales, defined by the spectral analysis, is well in agreement with the typical range of scales of the magnetospheric substorms, moreover *turbulence* has been considered, by now, as an important feature of the dynamics of *magnetosphere-ionosphere coupling* [23, 24]; hence it is possible to argue that probably the evolution of the substorms is characterised by *mixing* or *turbulence*.

Further studies are necessary in order to extend this analysis to other periods and in order to explain AE *multifractality* within a general *magnetospheric-ionospheric* model.

* * *

The authors are grateful to Prof. A. VULPIANI of the Università di Roma “La Sapienza” and to Dr. M. CANDIDI of Istituto di Fisica dello Spazio Interplanetario-CNR of Frascati (Rome) whose comments and suggestions have improved the final version on this paper. GC was financially supported by a fellowship of National Research Council (CNR). Financial support for this work was partially provided by the Italian National Project for Antarctic Research (PNRA).

REFERENCES

- [1] BURLAGA L., *Geophys. Res. Lett.*, **18** (1991) 69.
- [2] PRICE C. and PRICHARD D., *Geophys. Res. Lett.*, **20** (1993) 771.
- [3] PRICE C. and PRICHARD D., *Geophys. Res. Lett.*, **19** (1992) 1623.
- [4] ROBERTS D., *J. Geophys. Res.*, **96** (1991) 16031.
- [5] ROBERTS D., BAKER D. and KLIMAS A., *Geophys. Res. Lett.*, **18** (1991) 151.
- [6] SCHERTZER D. and LOVEJOY S., *J. Geophys. Res.*, **92** (1987) 9693.
- [7] SHAN L., HANSEN P., GOERTZ C. and SMITH R., *Geophys. Res. Lett.*, **18** (1991) 147.
- [8] SHARMA A., VASSILIADIS D. and PAPADOPOULOS K., *Geophys. Res. Lett.*, **20** (1993) 335.
- [9] TAKALO J. and TIMONEN J., *Geophys. Res. Lett.*, **21** (1994) 617.
- [10] TAKALO J., TIMONEN J. and KOSKINEN H., *Geophys. Res. Lett.*, **20** (1993) 1527.
- [11] VASSILIADIS D., SHARMA A., EASTMAN T. and PAPADOPOULOS K., *Geophys. Res. Lett.*, **17** (1990) 1841.
- [12] DAVIS T. and SUGIURA M., *J. Geophys. Res.*, **71** (1966) 785.
- [13] AKASOFU S., *Space Sci. Rev.*, **28** (1981) 121.
- [14] TSURUTANI B., SUGIURA M., IYEMORI T., GOLDSTEIN B., GONZALEZ W., AKASOFU S. and SMITH E., *Geophys. Res. Lett.*, **17** (1990) 279.
- [15] DAVIS A., MARSHAK A., WISCOMBE W. and CAHALAN R., *J. Geophys. Res.*, **99** (1994) 8055.
- [16] PALADIN G. and VULPIANI A., *Phys. Rep.*, **156** (1987) 147.
- [17] MENEVEAU C. and SREENIVASAN K. R., *Phys. Rev. Lett.*, **59** (1987) 1424.
- [18] HENTSCHEL H. and PROCACCIA I., *Physica D*, **8** (1983) 435.
- [19] HALSEY T., JENSEN M., KADANOFF L., PROCACCIA I. and SHRAIMAN B., *Phys. Rev. A*, **33** (1986) 1141.
- [20] KRAICHNAN R. H., *Phys. Rev. Lett.*, **65** (1990) 575.
- [21] ZHEN-SU SHE, *Phys. Rev. Lett.*, **66** (1991) 600.
- [22] BRISCOLINI M. and SANTANGELO P., *J. Fluid Mech.*, **270** (1994) 199.
- [23] LYSAK R. L. and DUM C. T., *J. Geophys. Res.*, **88** (1983) 365.
- [24] GOERTZ C. K. and BOSWELL R. W., *J. Geophys. Res.*, **84** (1983) 7239.